Beam loss and emittance growth of colliding proton beams in RHIC

W. Fischer, M. Bai, M. Harvey, ...

February 1, 2006

Abstract

The beam and luminosity lifetimes during the Run-5 polarized proton operation showed large variation from store to store. We report observed lifetimes and lifetime distributions. We calculate beam lifetimes and emittance growth due to luminosity, rest gas scattering, intrabeam scattering, and beam-beam elastic scattering.

1 Introduction

During the polarized proton Run-5 the beam and luminosity lifetimes showed large variations. Fig. 1 two stores with rather different luminosities, beam and luminosity lifetimes, and background signals. During the run the cause for the lifetime variations could not be conclusively identified. Below we summarize the beam and luminosity observations and compare them with beam lifetime and emittance growth calculations. We consider beam losses due to luminosity and rest gas scattering, and emittance growth due to intrabeam scattering, elastic rest gas scattering, and beam-beam elastic scattering. Tab. 1 list beam parameters for the Run-5 polarized proton operation. We restrict ourselves to stores at 100 GeV beam energy.

Table 1: Beam parameters at the beginning of the store during polarized proton operation in Run-5.

quantity	unit	operation
proton energy	GeV	100.0
relativistic γ	...	106.6
revolution time T	μs	12.8
bunches per beam N	...	56–111
bunch intensity N_b	10^{11}	0.39–1.05
norm. emittances ϵ_x, ϵ_y (95%)	mm mrad	8.2–43
transverse tunes (Q_x, Q_y),	...	(0.68,0.69)
rms bunch length	ns	2.8
number of head-on bb interaction n_{IP}	...	3
initial beam-beam parameter ξ/IP	..	0.0010–0.0057

- Need to introduce emittance definitions (trans. & long.)
- Need to introduce beam, emittance and luminosity lifetimes [8]
- Need to use consistent notation for emittances $\epsilon_{n,x,y,s}$
- Need to use consistent notation for lifetimes τ

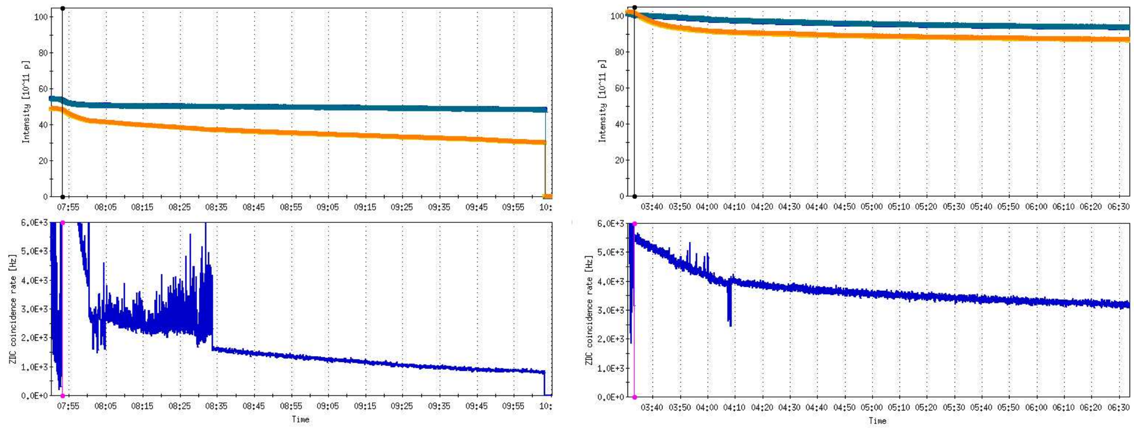

Figure 1: Beam intensities and PHENIX luminosity signal of two stores. Left, fill 7233, with moderate beam intensity in 58 bunches shows a poor Yellow beam lifetime, low initial luminosity, and a large background signal in the early part of the store. Right, fill 7327, has larger intensity in 106 bunches, and good beam and luminosity lifetimes. A change in the luminosity lifetime is visible after about half an hour, coinciding with a change in the Yellow beam lifetime.

2 Proton beam and luminosity lifetime observations in Run-5

2.1 Colliding beams

The time dependent proton intensities $N_b(t)$ of all physics stores (see Fig. 1) were fitted with either a single or double exponential function

$$N_b(t) = A_1 e^{-t/\tau_1} + A_2 e^{-t/\tau_2}. \tag{1}$$

Likewise, the time dependent luminosities $\mathcal{L}(t)$ of all physics stores (see Fig. 1) were fitted with either a single or double exponential function

$$\mathcal{L}(t) = A_1 e^{-t/\tau_1} + A_2 e^{-t/\tau_2}. \tag{2}$$

All fits start when the luminosity signal is free from background contamination. This can take up to half an hour after the beams were brought into collision. Background conditions were not reproducible either, and backgrounds at STAR were thought to correlate with horizontal orbit bumps in IP6. The STAR experiment had no shielding installed in Run-5.

In Fig. 2 the fitted Blue and Yellow beam lifetimes are shown. The left hand side show the fast decaying component, centered at 0.38 h and 0.41 h for the Blue and Yellow beam respectively. Both distributions are relatively narrow. The right hand side of Fig. 2 shows the slow decaying part. These distributions are much wider. A large number of Yellow stores have slow beam decay times of less than 50 h. The average slow decay times for the Blue and Yellow beam are 90 h and 57 h respectively. The beam lifetime of about one third of all physics stores could be well fit to a single exponential decay function, typically for both the Blue and Yellow beams. Most of these stores are in the early part of the run when the performance was still improving.

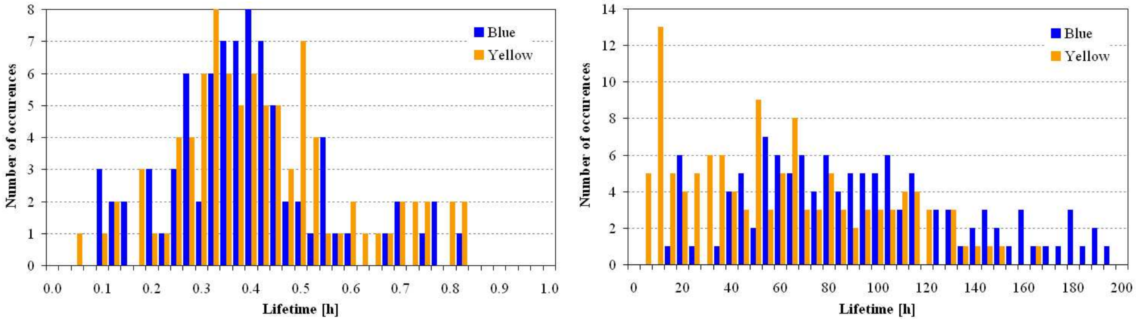

Figure 2: Beam lifetimes were fitted with a double-exponential function $N_b(t) = A_1 e^{-t/\tau_1} + A_2 e^{-t/\tau_2}$. Histograms of the fast (left) and slow (right) beam lifetimes components for the polarized proton physics stores of Run-5.

Fig. 3 shows the fast (left) and slow (right) luminosity lifetime distributions. The fast and slow components of the luminosity decay have average values of 0.3 h and 11 h respectively.

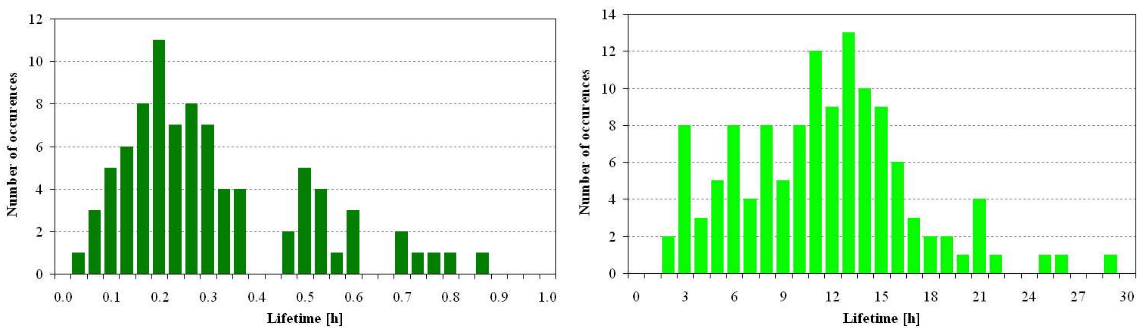

Figure 3: Luminosity lifetimes were fitted with a double-exponential function $\mathcal{L}(t) = A_1 e^{-t/\tau_1} + A_2 e^{-t/\tau_2}$. Histograms of the fast (left) and slow (right) luminosity lifetimes components for the polarized proton physics stores of Run-5.

2.2 Bunch length evolution

The rf voltage in store is 300 kV. The bunch length is measured with a wall current monitor. The FWHM of all bunches is averaged, and the time evolution of if fitted to a 3^{rd} order polynomial. The rms bunch length is calculated assuming Gaussian bunch shape.

The bunch length evolution of the Run-5 stores is shown in Fig. 5. The average Blue bunch length at the beginning of a store is 0.76 m. It increases by 20% to 0.91 m after 3 h. The average Yellow bunch length at the beginning of the store is 0.88 m, 16% larger than the Blue one. The average Yellow bunch length increases by 11% to 0.98 m after 3 h. A systematically larger Yellow bunch length has also been observed with Cu beams.

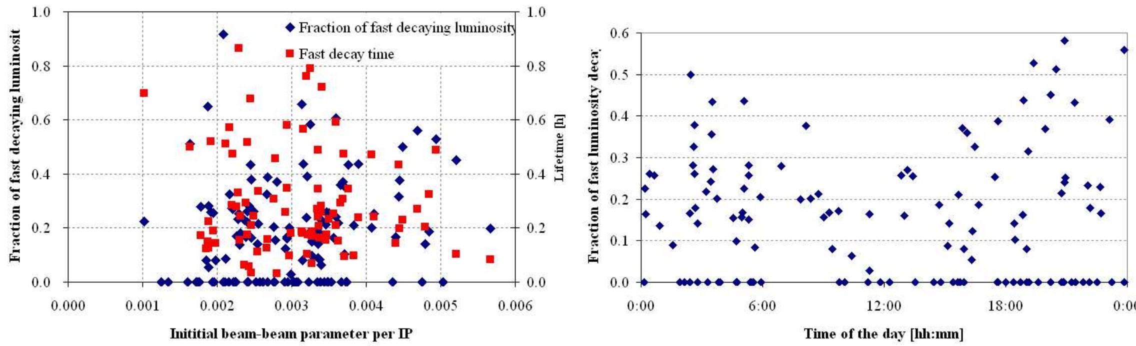

Figure 4: Luminosity lifetimes were fitted with a double-exponential function $\mathcal{N}(t) = A_1 e^{-t/\tau_1} + A_2 e^{-t/\tau_2}$. Left: fraction of the luminosity that decays fast $A_2/(A_1 + A_2)$ as a function of the initial beam-beam parameter ξ per IP. Right: Fraction of the luminosity that decays fast as a function of the time-of-the-day. A number of stores, particularly in the early part of the run, have no fast decaying component.

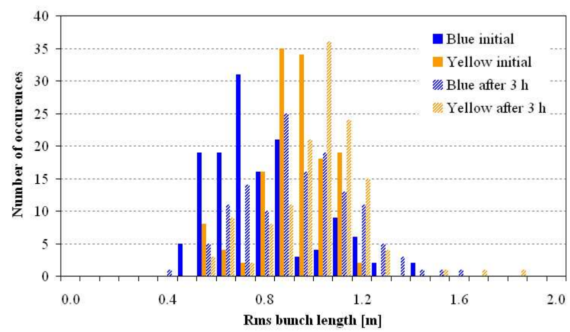

Figure 5: Rms bunch length at the beginning of stores, and 3 h later.

2.3 Beam-beam interaction

See Fig. 6.

2.4 Triplet magnetic field errors

The nonlinear magnetic field errors in the triplets are corrected with a beam-based method that minimizes the tune shift due to a local orbit bump [7].

The RHIC orbit undergoes diurnal vertical oscillations [3], likely to be caused by triplet moving with daily temperature variations. The vertical angle at IP6 was found to be a good representative of these orbit movements, and the IR4 triplets were identified as the main source [4]. The angle excursions at IP6 reached a maximum around 5am and 5pm every day.

The right-hand side of Fig. 4 shows the fast decaying part of the luminosity as a function of the time of the day. When the IP6 angel bump due to the diurnal orbit motion is near a maximum, the fraction of the luminosity that is decaying fast is increased. As similar plot for copper stores does not show any dependence on the time of the day. The total beam-

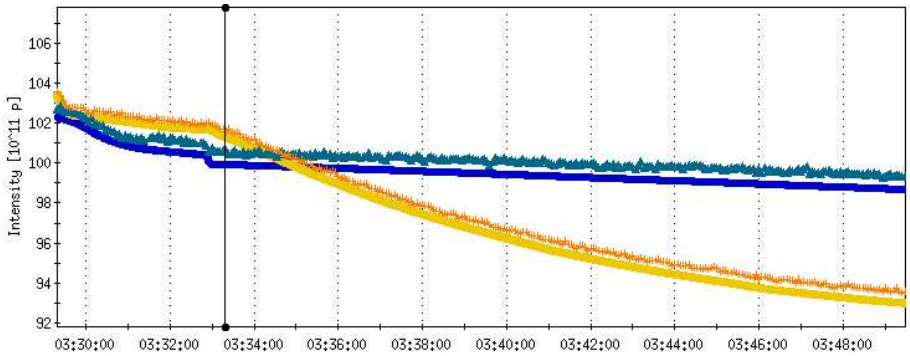

Figure 6: Effect of the beam-beam interaction on the beam lifetime at the beginning of the store. The vertical line marks the time when beams are brought into collision. In most cases the Yellow beam lifetime deteriorated visibly, in some cases the Blue beam lifetime became worse.

beam induced tune spread with copper beams (4 head-on collisions with $\xi \approx 0.0025$/IP) is close to the total beam-beam induced tune spread of proton beams (3 head-on collisions with $\xi \approx 0.0040$/IP). However, proton beams are about 50% larger in the triplet due to the same β^* at lower rigidity, and are thus more susceptible to nonlinear magnetic field errors in these locations.

— Fig. from Fulvia: triplet correctors on and off —

2.5 Single beams

at 100 GeV, at injection

2.6 Bunch length increase

3 Beam loss and emittance growth estimates

3.1 Average pressure calculations

To calculate beam loss and emittance growth from rest gas scattering, the average pressure is needed. We assume that only the warm RHIC regions contribute to beam loss and emittance growth. The pressure distribution in the warm sections is uneven.

3.2 Beam loss from luminosity

In Ref. [2] a total cross sections σ_{tot} and elastic cross sections σ_{el} are given for proton-proton collisions over a large range of energies. For beam energies of 100 GeV and 250 GeV respectively, the numbers shown in Tab. 2 can be extracted.

Table 2: Beam loss and emittance growth calculations for proton-proton collisions in RHIC. All parameters are for the beginning of store. The Run-5 parameter are close to the best stores achieved. The Enhanced RHIC I and RHIC II parameters are design goals.

parameter	unit	Run-5	Enhanced RHIC I		RHIC II	comment
main beam and lattice parameters						
proton energy E	GeV	100	100	250	250	
relativistic γ	...	— 106.6 —		— 266.4 —		
revolution frequency f_{rev}	kHz	— 78.2 —				
bunch intensity N_b	10^{11}	1.0	— 2.0 —			
bunches per beam N	...	— 111 —				
normalized emittance ϵ_n (95%)	mm·mrad	30	— 20 —		12	
envelope function at IP β^*	m	— 1.0 —			0.5	
rms beam size at IP $\sigma^*_{x,y}$	mm	0.22	0.18	0.11	0.06	
rms angular spread at IP $\sigma'^*_{x,y}$	mrad	0.22	0.18	0.11	0.12	
gap voltage V_{gap}	MV	— 0.3 —		— 3.0 —		
normalized bunch area S (95%)	eV·s	1.9	— 1.0 —			
rms bunch length σ_s	m	0.8	0.6	— 0.15 —		
rms momentum spread σ_p	10^{-3}	0.4	0.3	— 0.4 —		
hour-glass luminosity factor	...	0.81	0.88	1.0	0.96	
luminosity $\mathcal{L}$/IP	10^{30}cm^{-2}s^{-1}	15	90	220	750	
number of IPs n_{IP}	...	3	— 2 —			
beam-beam parameter ξ/IP	...	0.0025	— 0.0074 —		0.0123	
warm vacuum sections						
length per ring l_w	m	— 652 —				
average pressure $\langle P \rangle$	nTorr	— 30 —				
static gas composition	...	— 95% H_2, 5% CO —				
average β-functions $\langle \beta_{x,y} \rangle$	m	128	— 112 —		173	
beam loss from luminosity						
total p–p cross section σ_{tot}	mb	— 50 —		— 60 —		Ref. [2], interpolated
beam lifetime τ	h	1400	700	230	70	Eq. (6)
beam loss from rest gas scattering						
cross section $\sigma_{\mathrm{H_2}}$ for loss on H_2	b	— 0.231 —				Ref. [12]
cross section σ_{CO} for loss on CO	b	— 1.526 —				Ref. [12]
total cross section σ for beam loss	b	— 0.296 —				weighted average
beam lifetime τ	h	— 191 —				Eq. (8)
emittance growth from intrabeam scattering						
transverse emittance growth time $\tau_{x,y}$	h	255	33	13	4.1	BETACOOL [14]
longitudinal emittance growth time τ_s	h	20	2.2	3.9	2.0	BETACOOL [14]
emittance growth from rest gas elastic scattering						
coefficient	Torr^{-1}s^{-1}	— 0.05 —				10% H_2, 90% N_2
transverse emittance growth time $\tau_{x,y}$	h	27	21	52	20	Eq. (10)
emittance growth from beam-beam elastic scattering						
elastic p–p cross section σ_{el}	mb	— 8 —		— 9 —		Ref. [2], extrapolated
parameter b	(GeV/c)$^{-2}$	— 11.9 —		— 12.4 —		Eq. (15)
rms scattering angle θ_{rms}	mrad	— 2.1 —		— 0.8 —		Eq. (13)
emittance growth time $\tau_{x,y}$	h	6600	2200	5100	1836	Eq. (11)
total calculated lifetimes						
beam lifetime τ	h	172	148	105	53	luminosity, rest gas
transverse emittance growth time $\tau_{x,y}$	h	24	13	10	3.4	IBS, rest gas, el. BB
luminosity lifetime $\tau_{\mathcal{L}}$	h	19	11	8.6	3.0	all of the above

To make an estimate for the luminous beam and luminosity decay we assume that all particle interactions due to the total proton-proton cross section lead to the loss of both protons involved, and that there is no emittance growth. The particle loss per beam is then

$$n_{IP}N\frac{dN_b}{dt} = -\mathcal{L}(t)\sigma_{tot} \tag{3}$$

where n_{IP} is the number of interaction points, N the number of colliding bunches, and N_b the bunch intensity. For round beams the luminosity per interaction point $\mathcal{L}(t)$ is

$$\mathcal{L}(t) = \frac{3}{2\pi}(\beta\gamma)\frac{f_{rev}N}{\epsilon_n\beta^*}N_b^2(t), \tag{4}$$

which leads to a solution for $N_b(t)$ and $\mathcal{L}(t)$ of

$$N_b(t) = \frac{N_{b,0}}{1+t/\tau} \quad \text{and} \quad \mathcal{L}(t) = \frac{\mathcal{L}_0}{(1+t/\tau)^2} \tag{5}$$

with $N_{b,0} = N_b(0)$, $\mathcal{L}_0 = \mathcal{L}(0)$, and

$$\tau = \frac{NN_{b,0}}{n_{IP}\mathcal{L}_0\sigma_{tot}} = \frac{2\pi}{3(\beta\gamma)}\frac{\epsilon_n\beta^*}{n_{IP}f_{rev}N_{b,0}\sigma_{tot}} \tag{6}$$

Calculated lifetimes are in Tab. 2. These are much larger than the observed beam lifetimes in Run-5.

3.3 Beam loss from rest gas scattering

The beam loss from rest gas scattering leads to an exponential intensity decay

$$N_b(t) = N_b(0)e^{-t/\tau} \tag{7}$$

with

$$\frac{1}{\tau} = \frac{1}{N_b}\frac{dN_b}{dt} = -\frac{P_{av}}{kT}l_w f_{rev}\sigma_{rg} \tag{8}$$

where P_{av} and l_w are the average pressure and length of the warm sections respectively, and σ_{rg} the inelastic scattering cross sections. Ref. [12, 13]

- Need to include pressure variations around the ring.
- Need to calculate proper average $P\beta$
- Need to calculate cold arc contributions [16]

3.4 Emittance growth from intrabeam scattering

Fig. 7 shows the intensity of a store of 6 bunches in the Yellow, without collisions. The beam lifetime can be fitted to an exponential decay with a decay time of 35 h.

$$\frac{1}{\tau_{x,y,s}} = C_{x,y,x}\frac{N_b}{\gamma\epsilon_x\epsilon_y\epsilon_s} \tag{9}$$

Calculations with BETACOOL [14, 15].

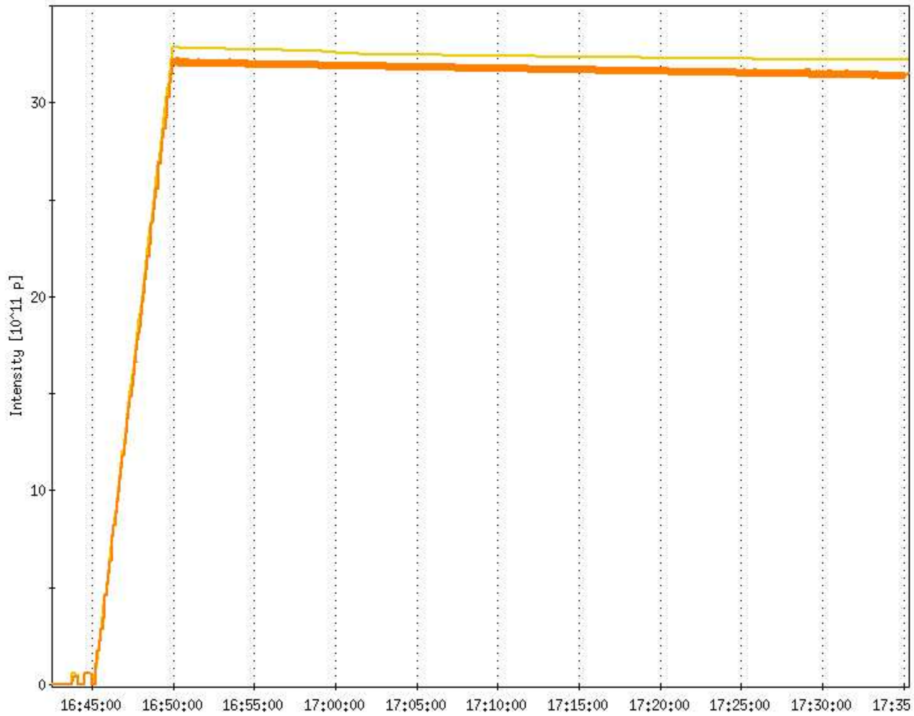

Figure 7: .

- Need to check calculations with MAD-X

3.5 Emittance growth from restgas elastic scattering

Approximately 700 m or each ring consist of warm vacuum pipes. In these the pressure typically does not exceed 10^{-7} Torr at the beginning of a store. The dynamic pressure decays to 10^{-8} to 10^{-9} Torr during the course of a store. The cold vacuum should not contribute to the emittance growth due to rest gas scattering, although increase gas densities were found with very high intensity beams [6].

The emittance growth due proton beam scattering with the residual gas, (assumed to be 10% H_2, 90% N_2), gives [8]

$$\frac{1}{\tau_{x,y}} = \frac{1}{\epsilon_n}\frac{d\epsilon_n}{dt} \approx 0.05\ \mathrm{Torr}^{-1}\mathrm{s}^{-1}\frac{\langle \beta P \rangle}{\gamma \epsilon_n}\frac{l_w}{C}, \tag{10}$$

where C is the circumference of the machine.

- Need to get calculation for actual gas composition (under dynamic conditions), coefficient from Eq. (12) in Ref. [8], coefficient from Eq. (13) in Ref. [5] appear to be different [not clear what units are required for input parameters in all cases]
- Need to include pressure variations around the ring.
- Need to calculate proper average $P\beta$

Table 3: Locations and average β-functions of the RHIC warm sections. $\beta^* = 1.0$ m and $\beta^* = 0.5$ m is only be possible in IR6 and IR8, where also the rotators are located. β-functions are given for one side of the IR. Due to the anti-symmetry of the IR optics, β_x and β_y are exchanged on the other side.

section	sections per ring	location from IP [m]	section length [m]	$\langle\beta_{x,y}\rangle$ [m]	$\langle\beta_{y,x}\rangle$ [m]
				— $\beta^* = 10.0$ m —	
IP–D0	12	0–20	20	30	30
Q3–rotator (IR6 & IR8)	4	38–60	22	21	85
Q3–Q4	8	38–76	38	23	63
Q7–Q8 (injection)	1	114–126	12	26	28
Q9–D9 (injection)	1	142–150	8	16	35
				— $\beta^* = 1.0$ m —	
IP–D0	12	0–12	20	200	200
Q3–rotator (IR6 & IR8)	4	38–60	22	197	724
Q7–Q8 (injection)	1	114–126	12	24	24
Q9–D9 (injection)	1	142–150	8	16	35
				— $\beta^* = 0.5$ m —	
IP–D0	12	0–20	20	400	400
Q3–rotator (IR6 & IR8)	4	38–60	22	322	1160
Q7–Q8 (injection)	1	114–126	12	26	25
Q9–D9 (injection)	1	142–150	8	17	18

- Need to calculate cold arc contributions [16]

3.6 Emittance growth from beam-beam elastic scattering

The emittance growth due to beam-beam elastic scattering at a single IP is [5]

$$\frac{1}{\tau_{x,y}} = \frac{1}{\epsilon_n}\frac{d\epsilon_n}{dt} = \frac{9}{2}\gamma n_{IP}\frac{f_{rev}N_b}{\epsilon_n^2}\sigma_{el}\langle\theta_{rms}^2\rangle \tag{11}$$

where θ_{rms} is the rms scattering angle. At high energies, the differential cross section is well described by a simple exponent [8, 9]

$$\frac{d\sigma}{dt} \sim e^{-b|t|} = \exp\left\{-\frac{\theta^2}{2\langle\theta_{rms}^2\rangle}\right\} \tag{12}$$

where $t \approx -p^2\theta^2$ is the square of the 4-momentum, and p the proton momentum. The rms scattering angle is then

$$\theta_{rms} = \frac{1}{p\sqrt{2b}}. \tag{13}$$

The parameter b can be calculated in the momentum range from 5 GeV/c to many TeV/c according to [10, 11]

$$b(p) = b_0 + b_1\sqrt{\frac{p_0}{p}} + b_2\ln\left(\frac{p}{p_0}\right) \tag{14}$$

with fitted parameters b_0, b_1, and b_2 from Ref. [10]:

$$
\begin{aligned}
p_0 &= 1\ (\mathrm{GeV}/c) && (15)\\
b_0 &= +11.13 \pm 0.22\ (\mathrm{GeV}/c)^{-2} && (16)\\
b_1 &= -6.21 \pm 0.53\ (\mathrm{GeV}/c)^{-2} &&\\
b_2 &= +0.30 \pm 0.04\ (\mathrm{GeV}/c)^{-2}. &&
\end{aligned}
$$

Calculated values for b, θ_{rms} and the emittance growth rate are shown in Tab. 2. Note that the rms scattering angles are much larger than the rms angular spread of the beam. Almost all scattered particles will therefore be lost at the collimators. The lost particles are accounted for in the beam loss from luminosity in Sec. 3.2, that uses the p–p total cross section σ_{tot}. The emittance growth due to this effect can be neglected.

4 Other issues

- What are the important machine nonlinearities at 100 GeV? Triplet errors, ...
- What is the evidence that these nonlinearities are important at 100 GeV?
- Effect of 10 Hz vibrations and modulated IP offsets.

Studies/data required

- Lifetimes and emittance growth: Single beam at 100 GeV at low beta (* = 1m) - with nominal intensities and emittances and fresh beams if possible, both rings
- Single beam lifetimes and emittance growth at 100 GeV at injection beta (* = 10 m), both rings (this will help determine the impact of triplet errors)
- Any other useful data from stores - e.g. tune evolution, ...

5 Summary

...

6 Acknowledgments

The authors are thankful to A. Fedotov, N. Mokhov, T. Roser, V. Ptitsyn, T. Sen, operations teams.

References

[1] W. Fischer, “RHIC run overview”, http://www.agsrhichome.bnl.gov/RHIC/Runs/ (2005).

[2] S. Eidelman et al., Phys. Lett. B 592, 1. Fig. 40.11 (2004) and 2005 partial update for the 2006 edition available on the PDG WWW pages (URL: http://pdg.lbl.gov/); Data courtesy of COMPASS group, IHEP, Protvino (August 2005).

[3] V. Ptitsyn, "Orbit mysteries: clues and cures", RHIC Retreat, June 2005, http://www.c-ad.bnl.gov/RHIC/Retreat2005/ (2005).

[4] D.Trbojevic, D. Bruno, V. Ptitsyn, P. Thieberger, private communication (2005).

[5] M. Syphers, "Emittance dilution effects [1]", in "Handbook of accelerator physics and engineering", World Scientific, (1998).

[6] D. Weiss, H.C. Hseuh, "Vacuum and NEG pipes", RHIC Retreat, June 2005, http://www.c-ad.bnl.gov/RHIC/Retreat2005/ (2005).

[7] F. Pilat, Y. Luo, N. Malitsky, and V. Ptitsyn, "Beam-based nonlinear optics corrections in colliders", proceedings of the 2005 Particle Accelerator Conference, Knoxville, TN (2005).

[8] N.V. Mokhov and V.I. Balbekov, "Beam and luminosity lifetime", in "Handbook of accelerator physics and engineering", World Scientific, (1998).

[9] R. Rubinstein, "Total, elastic and diffractive cross sections at high energies", FERMILAB-Conf-90/160-E [E-710] (1990).

[10] J.P. Burq, M. Chemarin, M. Chevallier, A.S. Denisov, C. Doré, T. Ekelöf, J. Fay, P. Grafström, L. Gustafsson, E. Hagberg, B. Ille, A.P. Kashchuk, G.A. Korolev, A.V. Kulikov, S. Kullander, M. Lambert, J.P. Martin, S. Maury, M. Querrou, V.A. Verbeken and A.A. Voobyov, "Soft π^-p and pp elastic scattering in the energy range 30 to 345 GeV", Nucl. Phys. B 217 pp. 285-335 (1982).

[11] N. Mokhov, private communication (2006).

[12] D. Trbojevic, W. Fischer, H.-C. Hseuh, W.W. MacKay, and S.Y. Zhang, "Comparison between the predictions and measurements for the beam gas interactions during the last gold and proton runs in RHIC", proceedings of the 2002 European Particle Accelerator Conference, Paris, BNL-69006 (2002).

[13] D. Trbojevic, "The beam lifetime and emittance growth in RHIC under normal operating conditions and with a hydrogen gas jet", BNL RHIC/AP/136 (1997).

[14] I. Meshkov, A. Sidorin, A. Smirnov, E. Syresin, and G. Trubnikov, BETACOOL program, http://Lepta.jinr.ru/betacool.htm (1996-2006).

[15] A. Fedotov, private communication (2006).

[16] B. Jeanneret and F. Zimmermann, "What is an acceptable vacuum pressure in the LHC arcs?", proceedings of the First CARE-HHH-APD Workshop on Beam Dynamics in Future Hadron Colliders and Rapidly Cycling High-Intensity Synchrotrons (HHH-2004), CERN, Geneva, Switzerland, CERN-2005-006 (2005).